Journal of Marine Research, 57, 671–691, 1999

Wind-driven mixed layer and coastal upwelling processes off the south coast of South Africa

by Eckart H. Schumann[1]

ABSTRACT

Most coastal mixed layer and upwelling investigations have concentrated on the more important fisheries regions situated on the west coasts of the continents, while this paper analyzes conditions on the zonally-orientated south coast of South Africa. Most of the data originate from a short measurement program in the southern summer of 1995, involving both CTD measurements from a small boat and data from a temperature array and coastal sea surface temperature (SST).

Limited mixed layer statistics are derived and yield results similar to those of Lentz (1992), although a lack of current measurements precludes any assessment of the Ekman drift. It is shown that the nature of the summer wind forcing is very different to the situation off the South African west coast, with wind variability occurring on much shorter time scales from 2 to 6 days: this has important consequences for plankton blooms and is a likely reason why production is not as efficient off this coast. Past results (Tilney *et al.,* 1996) have shown the importance of coastal trapped waves at depth, but it is apparent that very different conditions occur near the surface.

It is found that the coastal SST is a very good monitor of wind-forced coastal upwelling conditions, probably because of the abrupt topography. Substantial baroclinic tidal signals are also apparent at times in the temperature measurements.

1. Introduction

Wind-driven coastal upwelling forms the physical basis of many of the world's major fishing areas in mid-latitude ocean basins. These generally lie off the west coasts of the continents, where equatorward winds cause offshore Ekman transport and the associated upwelling of nutrient-rich waters. Because of the commercial importance of the fisheries, and the consequent need to understand and manage the systems, extensive research efforts have resulted in some areas. In particular, detailed upwelling investigations have been undertaken off the coasts of California, Peru and NW Africa (Brink, 1983; Lentz, 1992).

Another important upwelling fishery is situated in the Benguela system off the west coast of southern Africa (Shannon, 1985). It has also been subjected to intensive research, particularly in terms of the various biological components and management strategies; productivity and sustainable yields (e.g. Hutchings, 1992). Physical processes, particularly those directly associated with the fisheries, have formed an important component of these

1. Department of Geology, SAB Institute for Coastal Resource Management, University of Port Elizabeth, P.O. Box 1600, 6000 Port Elizabeth, South Africa. ***email: ocaehs@upe.ac.za***

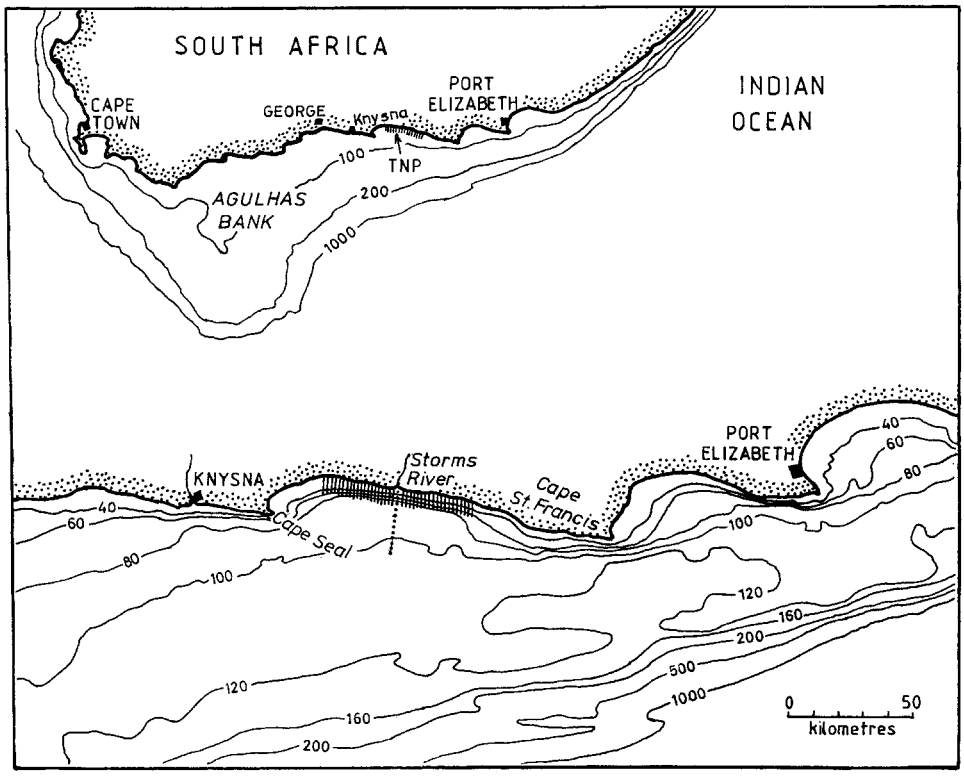

Figure 1. Map of the south coast of South Africa, with a larger scale section showing the area where the measurements were made. The position of the Tsitsikamma National Park (TNP) marine reserve is shown hatched, while the line of boat stations is indicated by the dotted line. The bathymetry is given in meters.

investigations (e.g. Shannon *et al.,* 1992); however, mixed layer dynamics have not been investigated to the same extent as those off California, Peru and NW Africa.

Wind-driven coastal upwelling also occurs in other areas, and is a well-established fact along the south coast of South Africa (Schumann *et al.,* 1982, 1988; Walker, 1986). This region is shown in Figure 1, and abuts the wide Agulhas Bank; farther offshore the Agulhas Current is a major western boundary current flowing southwestward, but having only a limited influence at the coast (Schumann, 1998). It has been established that westward component winds are more common along the South African south coast in summer than in winter (Schumann and Martin, 1991). These winds generate the offshore surface Ekman flux initiating coastal upwelling, while the intense thermocline established on the wide Agulhas Bank in summer (Schumann and Beekman, 1984; Swart and Largier, 1987) means that the coastal upwelling can be readily identified in thermal infrared satellite imagery; Figure 2 shows such upwelling structures on two different occasions, and this will be

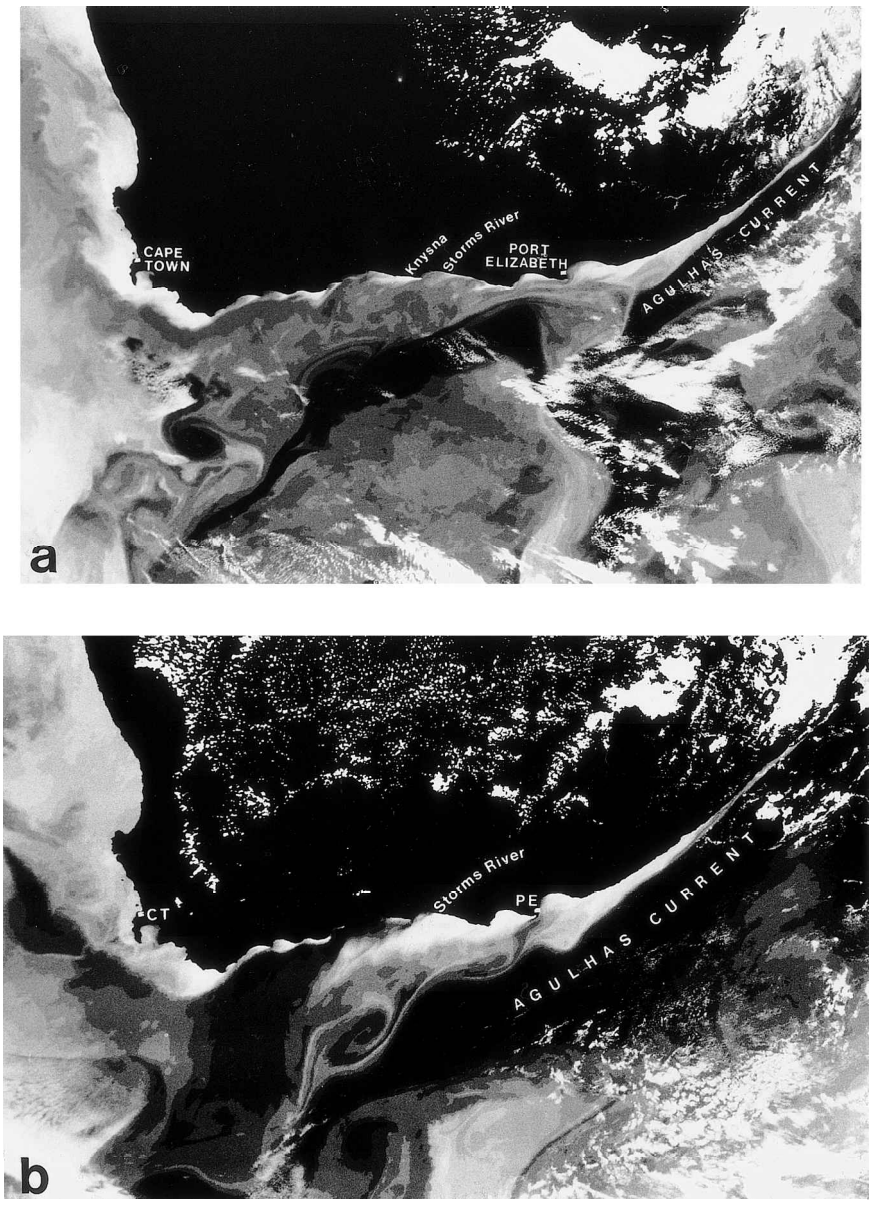

Figure 2. NOAA thermal infrared images on 26 March, 1987 (a), and 6 February, 1990 (b), depicting upwelling along the South African south coast. Colder water upwelled at the coast is shown in a whiter shade of grey. Note the large meander in the flow of the Agulhas Current in 1987, a feature occurring only occasionally (Schumann, 1998).

discussed further in the text. Preferential upwelling is initiated at the prominent capes, and then migrates westward and offshore with the upwelling alongshore current.

This analysis uses the results from a short measurement program in 1995 and seeks to characterize physical aspects of the South African south coast mixed layer and upwelling processes. The orientation of the coastline, zonal rather than meridional, is a major difference compared with the west coast (Fig. 1). It will be shown that the surface mixed layer structures are similar to those in typical west coast regions, but that wind forcing is significantly different, probably resulting in characteristically different upwelling regimes.

2. Data

The data analyzed here come primarily from a short investigation during the period January to May, 1995, at the Tsitsikamma National Park (TNP) marine reserve on the south coast of South Africa (Fig. 1). It is a reasonably straight section of approximately east-west coastline, with an abrupt coastal bathymetry extending to the general shelf depth of around 100 m within 10 km of the coast.

Six boat sections were completed during this period, using a small boat launched from the shore at the Storms River resort within the TNP, and covering a line of 13 stations extending to a distance of about 26 km offshore; not all the stations were completed on each section, and there were also slight differences in position. A *SeaBird* Electronics SeaCat was used at each station to obtain depth profiles of various parameters to a maximum depth of 58 m, limited by the instrument's depth capability. Only temperature profiles are of importance here since the average flow of the Storms River has a negligible influence, and salinities in the coastal areas of the Agulhas Bank vary little from oceanic values between about 35.3 and 35.6 (Lutjeharms *et al.,* 1996). Temperature values were obtained approximately every 0.5 m, with a calibrated accuracy better than 0.01 °C.

A thermistor string was deployed in a depth of 37 m about 1.5 km offshore of the Storms River mouth. This consisted of four Hobo temperature recorders situated at depths of approximately 8, 17, 27 and 36 m, with the given accuracy of these sensors better than 0.2 °C. The recorders were encased in plastic containers with a temperature response time of about 1 hour, and consequently the temperature recording interval was set at 1.2 hours. Three recorders have a full data return from 27 January to 16 May, while the fourth at a depth of 27 m only covered the period up to 16 February.

Over the same period as this experiment, coastal sea surface temperatures (SSTs) were measured in a well-flushed harbor on the inshore side of a small rocky promontory at the Storms River resort at 08:00, 14:00 and 20:00 with an accuracy of 0.1 °C. Prior to this, daily SST data were available from January, 1978, to September, 1989. Additional SST data for the south coast were also available farther westward at a well-exposed site in the Knysna estuary mouth over the period January, 1972 to July, 1992; these mid-morning measurements were made using a standard thermometer with an accuracy of 0.5 °C.

Wind data from four sites, namely Cape Town, George, Storms River and Port Elizabeth, are important and relevant to this investigation. Hourly measurements were made by the

South African Weather Bureau at the airports at Cape Town, George and Port Elizabeth using a Dines anemograph at a height of between 10 and 15 m; wind direction accuracy is given as 10° and speed as 0.1 m/s, with wind speed less than 1 m/s treated as calms. The coastal station at Storms River used RM Young wind speed and direction sensors mounted on a 10 m mast.

None of these wind measuring sites is ideal, with the airport sites all slightly inland and the Cape Town site affected by nearby mountains, and with the Tsitsikamma site at the foot of a coastal cliff. However, the results do allow analyses of the larger-scale weather patterns, and thus the identification of different features on the west and south coast. For the representations shown here, principal axes were calculated for the different sites, with the following results (angle in degrees from True North): Cape Town 167.6°; George 104.8°; Tsitsikamma 45.7° and Port Elizabeth 82.1°.

NOAA 9, 10 and 11 thermal infrared (TIR) satellite imagery was available for the South African coast from 1985 to 1992 on an approximately weekly basis, depending on cloud cover. SST contrasts allow the identification of upwelling structures, though the resolution is not sufficient to enable any detailed analyses to be performed.

3. Surface mixed layer

Lentz (1992) has performed a detailed analysis of the surface mixed layer structure off the coasts of California, Peru and northwest Africa. The particular aspect of importance in this analysis is the detail of the measurements made in the upper 20 to 30 m of the water column, using both moored current and temperature recorders, and conductivity/temperature/depth (CTD) profilers. The measurements from the South African south coast detailed here are by no means as comprehensive, but do nonetheless allow some comparisons to be made.

Figure 3 shows the six sections measured off the Storms River mouth, and the abrupt bathymetry and offshore temperature structure is clearly evident over the summer and early fall period. As expected, the thermocline during the January and February cruises was more intense than during March and April, which is an indication of the changeover to more isothermal winter conditions (Schumann and Beekman, 1984). These measurements—a total of 68 boat stations—will be analyzed here; the upper thermistor string position was not sufficiently close to the surface to allow the mixed layer structure to be identified.

Well-mixed near-surface waters mean that there will be weak vertical gradients. If it is assumed that salinity variations are negligible, then the surface mixed layer can be defined as the maximum depth over which the observed temperature lies within some value ΔT of the water temperature at the surface. Lentz (1992) rather arbitrarily chose ΔT to be 0.02 °C for CTD observations and 0.05 °C for moored observations.

The data from the 68 stations were analyzed using values of ΔT of 0.02, 0.05 and 0.1 °C, and Table 1 gives the results of the mean mixed layer depth for each case. Also included is the temperature gradient immediately below the measured mixed layer, and as expected there was an abrupt decrease in temperature below the mixed layer. Nonetheless, the table

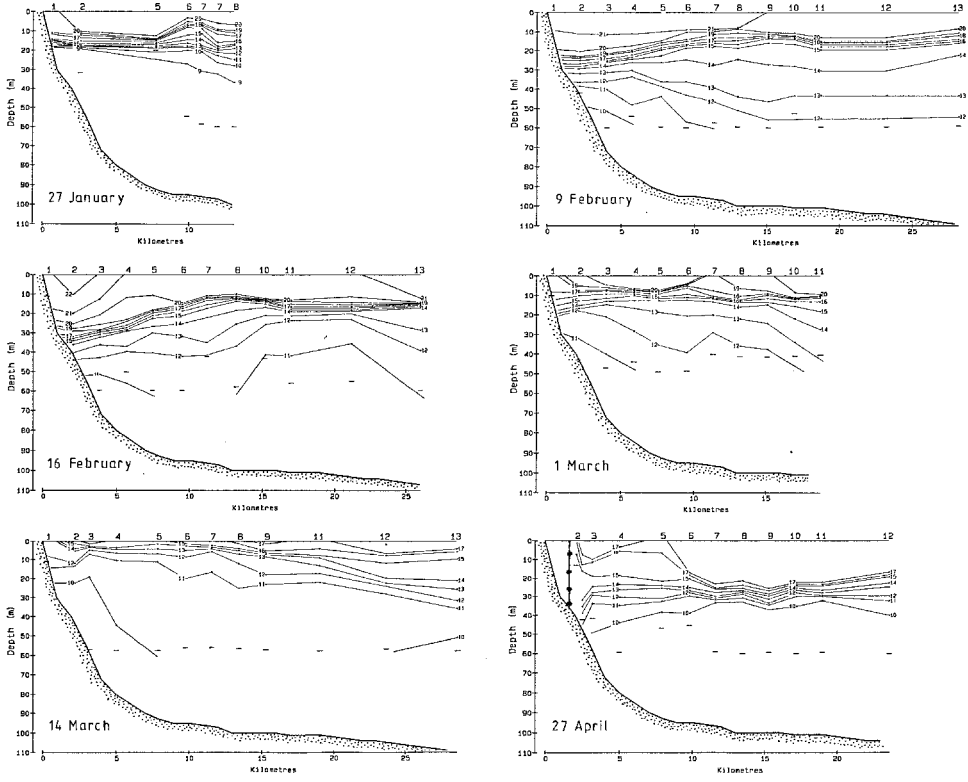

Figure 3. Temperature sections (in °C) from the six cruises undertaken in the period January to April, 1995. The lower limit of the profiles on each station is shown by a short line. The approximate positions of the sensors on the temperature array are shown on the section measured on 27 April.

also shows the mean of the maximum temperature gradient on each profile and the mean depth at this maximum gradient, and from this it is clear that the greatest thermocline intensity occurred well below what has been defined as the mixed layer depth. Of interest is the maximum thermocline intensity over all the cruises, of 2.8 °C/m.

Lentz's analysis showed that the mixed layer depth exceeded 10 m approximately 40% of the time at all the sites, and with means from the mooring data varying from 1.9 m to a

Table 1. Mean values of mixed layer depths, and the thermocline intensity immediately below the mixed layer, for different values of ΔT. The mean maximum thermocline intensity, and its depth, are also given.

ΔT (°C)	Depth (m)	Intensity (°C/m)
0.02	5.0	0.18
0.05	6.3	0.23
0.10	6.9	0.31
Maximum Intensity	14.8	1.29

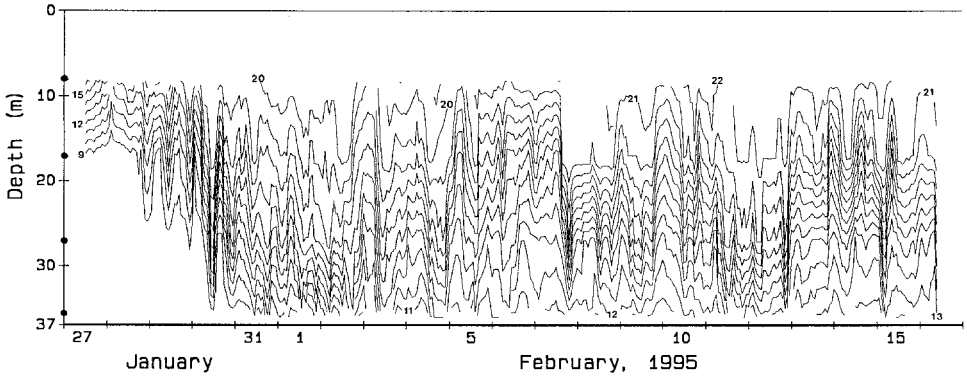

Figure 4. Time series of interpolated isotherms (in °C) from the temperature array. The sensors were located at depths of 8, 17, 27 and 36 m, which determine the depth limits of the diagram; these positions are indicated on the depth axis.

maximum of 13.7 m (off northwest Africa), but with most values below 10 m. The results given in Table 1 therefore fall well within this range.

4. Coastal and temperature array variability

Temperature variability takes place over a range of time scales, and the data from the array allow variability in the tidal and inertial range to be investigated. Figure 4 shows a time series of temperature variability using the 1.2-hourly records from all four recorders on the array over a period of 21 days. The data have been linearly interpolated to provide isotherms: this interpolation will not provide the correct vertical structure, but will demonstrate the time variability of the system.

It is clear that substantial oscillations occurred at these higher frequencies, extending from one sensor position to the next and therefore with amplitudes in excess of 5 m; this is in contradiction to the finding by Largier and Swart (1987) that the inner portion of the Agulhas Bank has negligible internal tides. In particular, the semidiurnal M_2 tide is evident during the last three days of January, and then again on 14 and 15 February, with an indication of such fluctuations at other times. These are not consistent or continuous oscillations, and are possibly associated with pulses of tidal energy propagating into the area. Largier (1987) reported the existence of such internal tidal pulses off the Cape peninsula farther to the west.

In order to confirm the tidal influence, spectra of the different temperature time series showed prominent peaks at the M_2 period of 12.42 hours; such analyses cannot give detailed information on the amplitude of the oscillations because of the vertical position of the sensor with respect to the thermocline. A broad peak in the spectra also occurred covering the diurnal tidal period (24 hours) and the inertial period (21.4 hours). Schumann and Perrins (1982) and much earlier Welsh (1964) have shown that inertial fluctuations are

important on the wider Agulhas Bank, and it is, therefore, not surprising that these records also show evidence of their existence.

These shorter period changes in the vertical position of the thermocline can also affect the measurement of sections such as those shown in Figure 3. A section typically took up to 3 hours to complete, which means that changes of 5 m or more in the position of isotherms could have been caused by these oscillations.

For further analysis these higher frequency oscillations were removed by filtering the different time series using a Cosine-Lanczos filter with 97 weights and a quarter power point at a frequency of 0.031 cycles per hour; this effectively removed oscillations with a period of less than about 30 hours.

Figure 5 shows the filtered data from three recorders on the temperature array and wind vectors measured at the Storms River site in the TNP; the measurements at the depth of 27 m were excluded because of the short data record. Also shown is the coastal SST record made at the Storms River site: these records were linearly interpolated to derive hourly values for easier comparison with the other data. It is clear that there was a close association of temperatures with wind, and that dramatic decreases in temperature occurred in the upper layers of the ocean after the onset of westward winds, with an increase in temperature with eastward winds. This is as expected, with westward component winds causing an offshore Ekman transport resulting in upwelling at the coast and conversely, eastward winds causing downwelling. Such associations are not new, and have been reported on numerous occasions elsewhere (e.g. Halpern, 1976; Brink *et al.,* 1983). The establishment of the Ekman drift in the upper layer is generally thought to occur within an inertial period (e.g. Gill, 1982), though it is important to note that mixed layer deepening due to wind stress reaches a maximum in a time scale of half an inertial period (Brink, 1983). Of interest is the occasional increase in bottom temperatures with downwelling, a process also reported at sites in deeper waters farther offshore (M. Roberts, pers. comm.).

A strong thermocline existed at the start of the experimental period in February, with surface temperatures of over 22 °C, and bottom temperatures at times less than 10 °C. However, there was a substantial decrease in near-surface temperatures from the end of February, and by mid-March almost isothermal conditions were evident. Thereafter the thermocline re-established itself, though with much lower coastal and surface temperatures, and consequently was much less intense. This is also reflected in the sections shown in Figure 3, where greater mixing is evident over the water column close to the coast, and on 14 March upwelling appears to have occurred leading to colder water over the whole water column at the coast.

A further important result from the temperature records shown in Figure 5 is the close correlation between the coastal SST measured at the Storms River site and the near-surface temperature records from the array. This is investigated further in Figure 6, which shows the coherency and phase between the coastal SST and the temperature measurements at 8 and 17 m depth, using the techniques described in Jenkins and Watts (1989). As expected

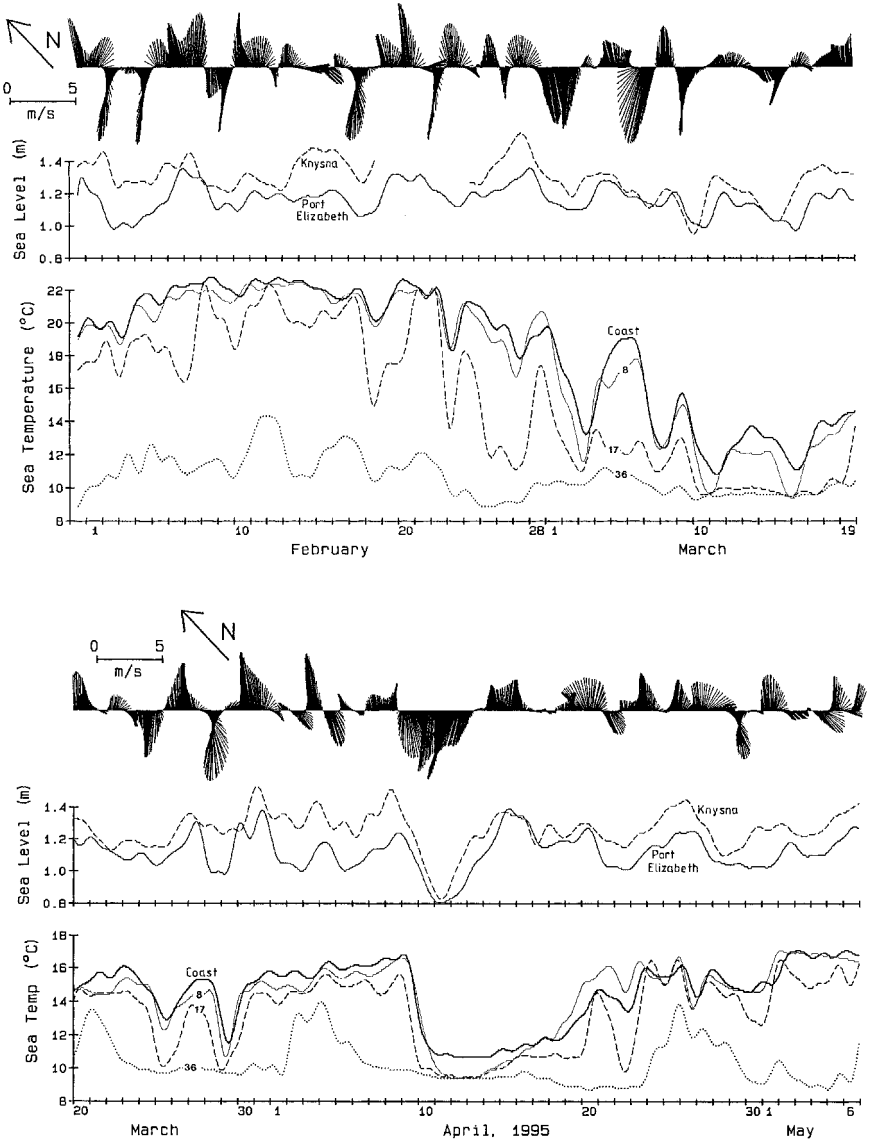

Figure 5. Time series of filtered wind vectors measured at the Tsitsikamma weather station, with filtered sea level from Knysna (dashed line) and Port Elizabeth (solid line), and filtered sea temperatures measured at the coast and at the indicated depths on the offshore array. Wind vectors are shown in the oceanographic sense; i.e., they point in the direction *to* which the wind is blowing; the orientation has been chosen such that the principal axes lies perpendicular to the time axis, and westward component winds point down on the page.

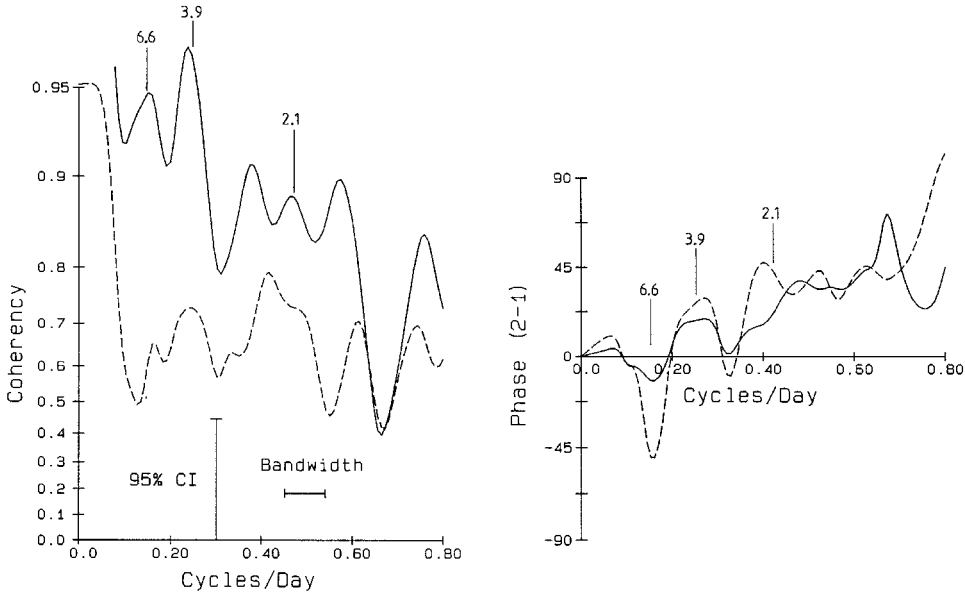

Figure 6. Coherency between the coastal SST measured at the Storms River resort and the temperature record at 8 m depth (solid line), and that from 17 m depth (dashed line). Note that on the arctanh scale the confidence interval is independent of frequency (Jenkins and Watts, 1968); the confidence limits are not shown on the phase diagram because they vary with the corresponding coherency. The period in days has been indicated above selected peaks in the spectrum.

from Figure 5 the coherency is very high, particularly between the coastal measurements and those recorded at 8 m depth, and to a lesser extent at 15 m depth.

At coherencies greater than 0.8, the 95% confidence limit on the phase angle is better than 10°. The phase diagram, therefore, indicates that at periods of about 6 days the temperature changes in the water column lead those at the coast by about 6 hours, while at the shorter periods the temperature changes at the coast lead those in the water column by about the same time; in practice it can be assumed that there is minimal difference. Note that the linear increase in phase angle with frequency means that the delay remains essentially constant with decreasing period.

It points to an essentially simple upwelling system where the offshore bathymetry is relatively abrupt, thus allowing the upwelling process to progress right to the coast itself; these structures are also reflected in Figure 3. The cross-shelf Ekman transport U_E is typically about 7 cm/s for a wind of 3 m/s (Schumann *et al.,* 1995), or 0.25 km/hour. This means it would take of the order of 6 hours to move offshore to the mooring site, in agreement with the delays found above. However, the exact nature of the temperature variability at depth will depend on the mixed layer structure and depth.

Past analyses have shown that wind-forced barotropic coastal trapped waves (CTWs) play an important role in the dynamics of this region (Schumann and Brink, 1990; Jury *et*

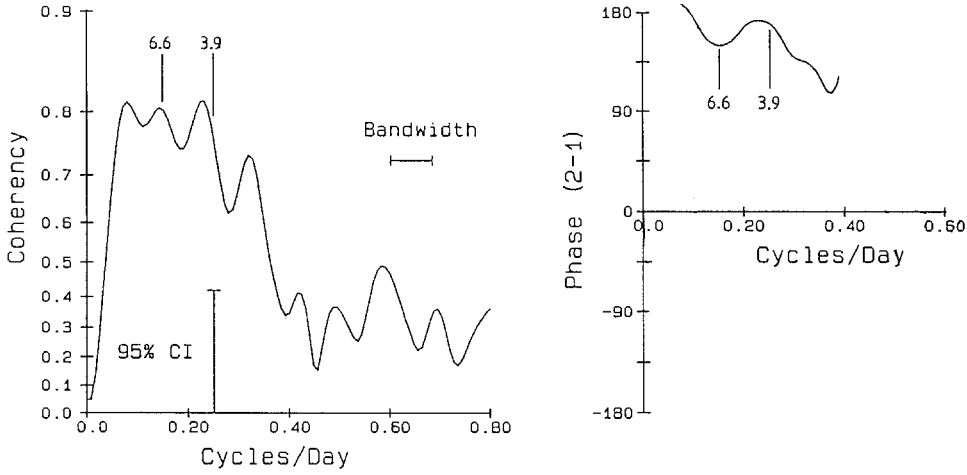

Figure 7. Coherency and phase between the major axis wind from Tsitsikamma and sea level measured in the harbor at Port Elizabeth. The phase is shown only where the corresponding coherency is greater than the 95% confidence limit.

al., 1990), and consequently sea level variability from tide gauges at Knysna and Port Elizabeth is also shown on Figure 5. The progression of the CTWs from west to east is clearly evident in the record, with a typical time delay of about 12 hours. The two sites are separated by about 250 km, and this gives a propagation speed of about 5.8 m/s, in good agreement with the results of Schumann and Brink (1990).

Schumann and Brink (1990) showed that the large amplitude of these waves along this coast is due to a condition of resonance or near-resonance between the wind systems propagating along the coast and the free-wave speed of the CTWs. As a result it can be expected that there should be a consistent association between the CTWs and the wind, and indeed it appears that the peaks of the CTWs tended to occur during westerly winds, with the troughs during easterly winds. This is investigated further in Figure 7, where a high coherence is established between the major axis wind from the Tsitsikamma site and Port Elizabeth sea level in the weather band from about 3 to 10 days. For periods less than 6.6 days the phase shows a lag less than 3 days, though up to about 10 hours would have resulted from the CTW propagation from Tsitsikamma to Port Elizabeth.

Tilney *et al.* (1996) present current meter data at a depth of 48 m in 51 m of water which show that at that depth barotropic CTWs are the dominant influence controlling current variability.

There is also a strong correlation in the temperature structure with sea level variability, with more homogeneous conditions occurring in the water profile at troughs in the sea level. However, this is more likely to be the result of on and offshore movement of water caused directly by the wind, since in theory the currents associated with the barotropic CTWs should be flowing parallel to the coast. At this stage there is no experimental evidence available for the existence of baroclinic CTWs.

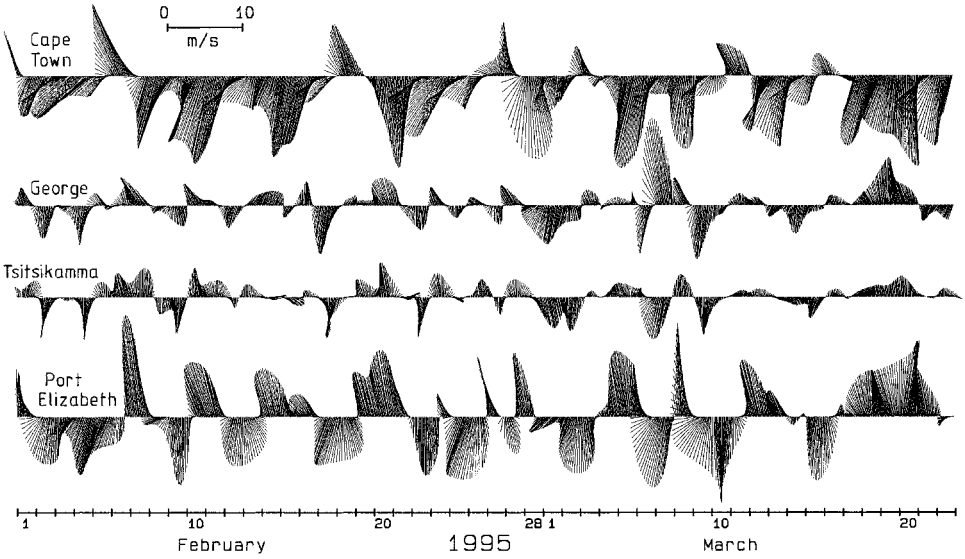

Figure 8. Time series of filtered wind vectors during February and March, 1995, as measured at Cape Town, George, Tsitsikamma (Storms River) and Port Elizabeth. The vectors are shown in the oceanographic sense; i.e., they point in the direction *to* which the wind is blowing, while the orientation has been chosen such that the principal axis at the various sites lies perpendicular to the time axis, and westward-component winds point toward the bottom of the page.

5. Wind-generated upwelling processes

It is important to investigate the periodicities associated with local wind fields at the TNP in greater detail, because there are significant differences along the south coast of South Africa compared with the better-known upwelling regions. Schumann and Martin (1991) reported that wind frequencies appear to be greater at south coast sites than along the South African west coast, and Figure 8 shows simultaneous wind measurements at Cape Town and three south coast sites, namely George, Tsitsikamma (Storms River) and Port Elizabeth.

It is clear in the time series shown in Figure 8 that wind variability occurred at longer periods on the west coast than on the south coast. The dominant winds in summer at Cape Town are the southeasterlies, i.e. northwestward, with percentage occurrence from November to March of more than 70% (Schumann and Martin, 1991), and it is apparent that they prevailed for relatively long periods: for example, around 10 February, 1995, the northwestward winds continued blowing for up to 10 days. On the other hand, the eastward winds remain dominant at Port Elizabeth even in summer, though comprising only marginally more than 50% at this season. Figure 6 tends to support this result, with the greater variability allowing a regular change in wind direction.

The short-term variability is evident at all the three south coast sites, with propagation of the wind systems from west to east: Schumann (1989) found speeds typically between 3

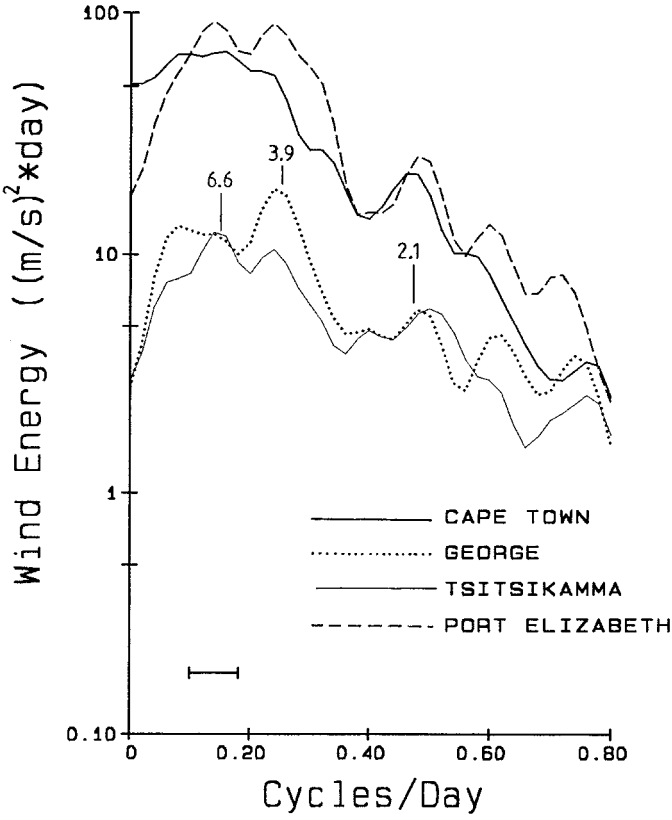

Figure 9. Autospectra of major axis winds from Cape Town, George, Tsitsikamma and Port Elizabeth.

and 8 m/s. Wind speeds at George and Tsitsikamma were generally considerably less than at Cape Town and Port Elizabeth.

The difference between the winds on the south coast and those on the west coast are further exhibited in the autospectra shown in Figure 9. Thus all the south coast spectra drop off rapidly at periods longer than about 6 or 7 days, while high energies are maintained at much longer periods at Cape Town. All the spectra have a trough at about 2.5 days, with another peak at 2 days; it is not clear how significant this distinction is. As expected, the spectral slope is flatter at the two south coast stations.

The autospectra also show the much lower energies in the wind field at George and Tsitsikamma expected from Figure 8. However, it must be recognized that winds over land are affected to varying extents by topography and land effects (e.g. Caldwell *et al.,* 1986; Hunter, 1982), and, therefore, winds at sea should be stronger, though the extent is unknown.

Preston-Whyte and Tyson (1988) have described the atmospheric circulation over

southern Africa, with the subtropical South Atlantic anticyclone dominating the southwest coastal weather. In summer the anticyclone ridges primarily south of the continent, setting up a gradient with the interior low that drives the strong southeasterly winds. The Cape south coast comes under the influence of the same large-scale weather patterns, but the greater variability probably originates in smaller-scale systems, in particular the so-called *coastal lows,* which are shallow systems generally less than 1000 m deep and with horizontal dimensions of the order of 100 km. Gill (1977) modeled these coastal lows as trapped waves in the atmosphere, being below the inversion layer, trapped against the coastal escarpment and propagating from west to east at theoretical speeds of about 20 m/s. He speculated that onshore or offshore winds generate these coastal lows.

Preston-Whyte and Tyson (1988) identified a typical 6-day weather pattern, while off the east coast province of KwaZulu-Natal. Hunter (1988) also found that the 3.8-day period was of marked significance. These periods have also been identified here, but it is apparent that this variability is not as marked on the west and southwest coasts of southern Africa. Thus, the coastal lows can be identified at the south coast sites, but with not such a clear link to Cape Town and the west coast. Estie (1984) reported that the coastal lows on the south coast are not the same as those on the west coast. Specifically, it appears that there are a greater number of coastal lows on the south coast, associated with the frontal systems that move eastward to the south of the subtropical anticyclone belt. Estie (1984) found different propagation speeds between fronts associated with the cyclonic belt and coastal lows on the south coast, and Schumann (1989) speculated that geostrophic coastal low systems could not be set up in the time that the larger air pressure systems took to traverse along the south coast. It means that the smaller-scale weather systems on the west coast are not the same as those on the south coast.

The relationship between winds and sea temperatures is investigated further in Figure 10. Here the strong correlation is confirmed for all three temperature series, namely at the coast and at the mooring at depths of 8 and 17 m. In fact while all three graphs are similar, they have different maxima at periods of about 6.6 days, 3.9 days and 2.1 days. It is not clear whether significance should be attached to this, since the depth of the thermistors in the ocean will determine their response. However, the fact that the coherence between the coastal SST and wind is greatest at a period of about 2.1 days does support the conclusion reached earlier that coastal SST is a good measure of upwelling events. The phases between winds and temperatures vary from about 70 to 110°, giving a time lag ranging from about 0.5 days to 4.5 days.

It can, therefore, be concluded that, for the abrupt topography on the south coast, the sea temperature measured at the coast is a good indication of upwelling in the adjacent ocean. Consequently, the average length of time that an upwelling event persists can be ascertained by determining the period between a drop in temperature at the coast at the initiation of the event and the subsequent rise in temperature when the wind stops blowing or reverses, and upwelling is terminated or downwelling occurs.

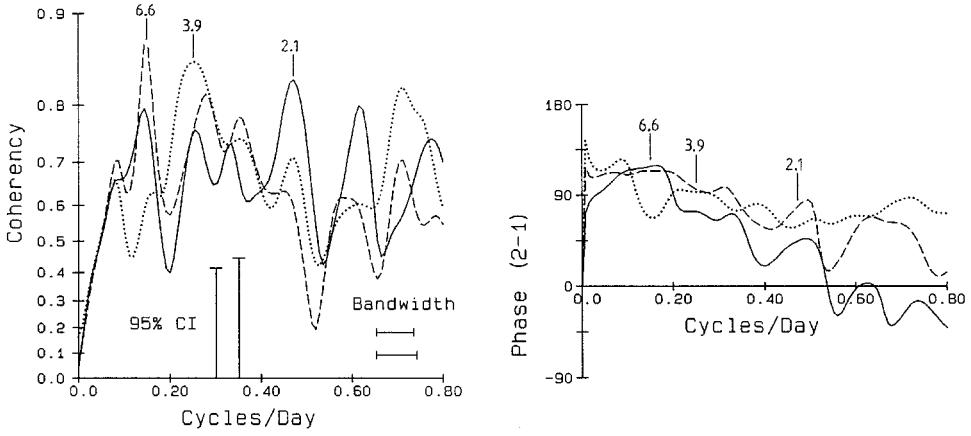

Figure 10. Coherency between the major axis wind from Tsitsikamma and SST measured at the coast, and the temperature recordings from the two upper position of the mooring at depths of 8 and 17 m. Note that the confidence interval and bandwidth are smaller for the longer coastal SST record.

The 11 years of Tsitsikamma coastal SST data, and 20 years of Knysna SST data can be used to test these periodicities further. Figure 11 shows the period in days between different decreases in temperature at the two coastal sites, and the subsequent rise in temperature; only the summer months from December to March have been used in the analysis. Note that in each case the rise in temperature has been taken to be slightly less than the drop, since some mixing would have occurred with the movement of the thermocline closer to the surface, and hence the contrast would have diminished.

Figure 11 lends confirmation that upwelling events on the Cape south coast are generally of short duration. At the TNP the maximum number of fluctuations in temperature occurred at periods of one day, with a rapid decrease in frequency of occurrence with increasing number of days, and very few events lasted longer than 4 days. There appear to be some differences at the Knysna site, with the maximum duration of upwelling events shifting to 2 days, but again very few lasted longer than 4 days. The actual frequency of occurrence at Knysna, and the limited number of upwelling events at 1 and 2 days, may have been due to the position of the measuring point inside the mouth of the estuary, which meant the cold water needed time to penetrate through to the site.

The picture that emerges of upwelling on the south coast is of fluctuating winds with periods ranging from about 2 to 6 days. These generate upwelling events over a typical period of a day, and because of the generally thin mixed layer, this is registered rapidly at the coast by a sharp drop in temperature, and at fixed points in the water column within a few kilometers of the coast. However, by that time the wind will have changed again, and the cold water events do not last longer than a few days.

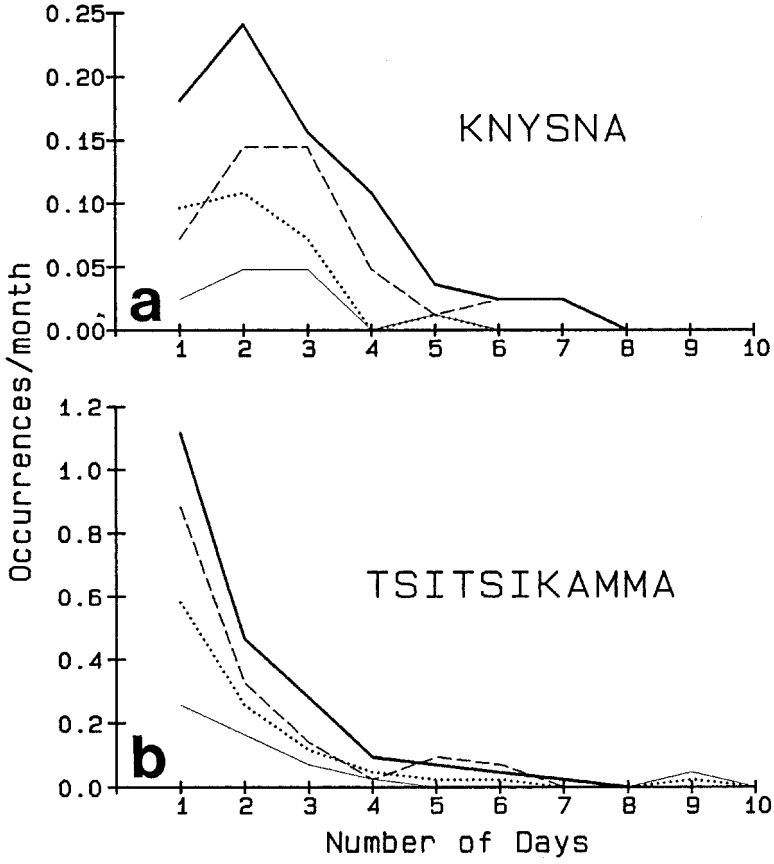

Figure 11. Relationship between the number of days between a specified drop in temperature, and then a subsequent specified rise in temperature, for (a) Knysna, and (b) Tsitsikamma (Storms River). The dark solid line is for a drop of at least 2°C over a period of one day, and then a subsequent rise of at least 1°C over one day, the dashed line for a drop of 3°C and rise of 1.5°C, the dotted line a drop of 4°C and a rise of 2°C, and the light solid line a drop of 5°C and rise of 2.5°C.

6. Discussion

Lentz established that a significant fraction (25% to 50%) of the wind-driven Ekman transport occurs below the surface mixed layer as he defined it; i.e., with ΔT no more than 0.02 for CTD observations and 0.05 for moored observations. It does mean that, if the mixed layer is taken down to the maximum intensity of the thermocline (Table 1), the Ekman transport should all lie within this depth. For the Tsitsikamma coast the Ekman flow would then generally be confined to the upper 15 m or so.

Upwelling fronts, in terms of sharp, near-surface horizontal density gradients, are well-established features associated with upwelling processes. The most intense gradients occur during the summer period when the seasonal thermoclines are established, and

according to Brink (1983) the reversing wind directions also play an important role in these dynamics. The fronts can form, move offshore and collapse in a fairly neatly defined cycle. Off Peru the winds are nearly always upwelling favorable, and the front then appears to remain far offshore and become relatively indistinct; the same conditions apply to the perennial upwelling cell off Hondeklip Bay in the northern section of the Benguela region (Nelson and Hutchings, 1983).

There has been considerable speculation on the nature of upwelling processes, and on the existence of complex, multicelled circulation structures (Brink, 1987). The limited offshore spatial detail means that these results cannot be used to investigate such features off the Tsitsikamma coast in detail, but the indications from Figure 3 are that multicelled upwelling is not a common feature of the Cape south coast. This may be because the short period between upwelling and subsequent relaxation or downwelling is not long enough to allow such features to develop.

This aspect of the wind-driven dynamics along the Cape south coast, namely the relatively short duration of the easterly and westerly component longshore winds, is one of the most significant results emanating from this analysis. It is in marked contrast to the situation found along most of the well-established upwelling regions lying along north-south coastlines off the west coasts of the continents.

Brink (1998) provides a basic formulation to describe the vertically integrated x and y components of the Ekman transport (U_E, V_E) in the presence of a wind stress $T \cos \omega t$ blowing in the y direction, namely

$$U_E = \frac{fT}{\rho\,(f^2 - \omega^2)} \cos \omega t$$

$$V_E = \frac{-\omega T}{\rho\,(f^2 - \omega^2)} \cos \omega t.$$

Here ω is the wind frequency, f the Coriolis parameter and ρ the water density. For most applications the low frequency limit ($f \gg \omega$) is applicable, which means that the alongshore Ekman transport $V_E \sim 0$, and correspondingly U_E is essentially perpendicular to the wind stress.

However, on the Cape south coast (~34S), $f \sim 8.2 \times 10^{-5}\ s^{-1}$, while for a wind variability period of two days $\omega = 3.6 \times 10^{-5}\ s^{-1}$, ranging to $1.2 \times 10^{-5}\ s^{-1}$ for six days. At these shorter periods V_E is small but not negligible, and is actually directed upwind but lags by a quarter of a cycle. Clearly it can be expected that the Ekman dynamics and consequently the upwelling processes will differ considerably from the standard formulations with longer-period wind variability.

The consequences for the biota in such rapidly fluctuating regions will also be very different to those in which more time is available for plankton blooms to develop. Hutchings (1992) reported that in excess of five days was necessary for the development of five different phytoplankton blooms on the South African west coast, and mismatching in

both time and space can occur between production of phytoplankton and zooplankton. Brink (1987) has emphasized the complexities inherent in frontal dynamics, and that a front is not a simple unbroken alongshore feature. Moreover, the decay of an upwelling front is not well understood and is dependent on the subsequent wind, with instabilities causing surface thermal patchiness. Subsurface chlorophyll patches also develop, and are dependent on upwelling processes, the depth of the euphotic zone, nutrient gradients and phytoplankton characteristics (Franks and Walstad, 1997).

It can then be expected that surface waters will be advected back and forth with the varying winds, but with mixing and instabilities ensuring that the system does not just oscillate between two states. Renewed upwelling will result in a new sequence, with the possibility of additional changes caused by seeding of newly upwelled water from past events (Hutchings, 1992). Moreover, where longshore currents have time to develop because of more consistent winds, it is possible that plankton can be lost from the system, whereas in a short-period oscillating system they may not move far before being brought back again.

The isotherm structure in Figure 3 indicates that upwelling did not progress much farther than 10 or 15 km offshore, and as stated earlier, there appears to be little evidence of multicelled upwelling. The available approximately 360 NOAA satellite images were inspected to ascertain whether upwelling progressed to any appreciable distance offshore, but there were few images showing the extensive upwelling along the coast as depicted in Figure 2b; even the upwelling as shown in Figure 2a did not occur often. It is of interest that the upwelling in Figure 2b extends eastward to the narrow shelf inshore of the Agulhas Current, where this major current is responsible for dynamically-driven upwelling which could then also influence conditions on the south coast (Schumann, 1998). As a comparison, on most images, particularly in summer, substantial upwelling was visible off the west coast.

Dispersion of larvae depend on their position within the water column, but it is apparent that seabed data will not reflect adequately the processes occurring in the surface mixed layer; moreover, the intense thermoclines experienced off the South African south coast in summer effectively inhibit transfer of materials across them. The current measurements analyzed by Tilney *et al.* (1996) show a progressive vector diagram in which substantial displacements caused by CTWs can occur at depths well below the thermocline, but it is also apparent that barotropic CTWs have little effect on the vertical temperature structure of the water column.

Hutchings (1992) considers the eastern Agulhas Bank as one of the three main areas of pelagic fish production around southern Africa. However, this primarily comprises the upwelling on the inner boundary of the Agulhas Current, and on the central part of the Agulhas Bank, and does not include the coastal upwelling discussed here. It would, therefore, appear that the efficiency of this southern coastal system does not compare with the western coastal upwelling systems, and is confirmed by the relative importance of the fisheries in the two systems. Nutrient levels are also much lower than those found on the

west coast (Lutjeharms *et al.,* 1996), but further inherent reasons for lower productivity need to be investigated in coordinated, multidisciplinary field investigations.

An interesting feature of upwelling along the Cape south coast is the temperature response at the coast itself, and the fact that upwelling variability can be determined from coastal SST variability; very few investigations elsewhere appear to have used such measurements in their analyses. As stated earlier, this is probably because of the abrupt topography along this section of coast and the limited interference of shallow-water effects close to the coast. However, it does mean that relatively easy measurements can be made of upwelling characteristics, in particular any alongshore spatial differences can be ascertained.

Schumann *et al.* (1995) found that in summer the SSTs along the south coast responded to relatively weak winds, also a confirmation of the fact that the mixed layer is shallow, with the abrupt topography allowing the signal to appear rapidly at the coast. They also investigated the interannual variability, in particular the effect of El Niño events. During El Niño years a smaller percentage of westward winds occurs, whilst during La Niña years there is a greater percentage and correspondingly average sea temperatures during summer are warmer and colder, respectively.

Acknowledgments. The use of National Parks Board facilities in the Tsitsikamma National Park is gratefully acknowledged. In particular, none of the measurements could have been made without the assistance and cooperation of John Allen, his crew, and the boat Aonix; Jon Churchill, Aiden Wood, Amanda McPhail and Wayne Ford are also thanked for helping on the six measurement cruises, and deployment of the temperature array. Moreover, Dr. Nick Hanekom is thanked for providing the daily measurements of sea temperature from Storms River, and Mr. C. Douglas for the daily temperature measurements at Knysna. The Weather Bureau provided wind data from Cape Town, George, Storms River and Port Elizabeth, while the Satellite Applications Centre of the CSIR provided the NOAA images. Funding for the project was provided by the South African Foundation for Research Development.

REFERENCES

Brink, K. H. 1983. The near-surface dynamics of coastal upwelling. Prog. Oceanogr., *12,* 223–257.

—— 1987. Upwelling fronts: implications and unknowns. S. Afr. J. Mar. Sci., *5,* 3–9.

—— 1998. Wind-driven currents over the continental shelf, *in* The Sea, K. H. Brink and A. R. Robinson, eds., *10,* 3–20.

Brink, K. H., D. Halpern, A. Huyer and R. L. Smith. 1983. The physical environment of the Peruvian upwelling system. Prog. Oceanogr., *12,* 285–305.

Caldwell, P. C., D. W. Stuart and K. H. Brink. 1986. Mesoscale wind variability near Point Conception, California during spring 1983. J. Climate Appl. Meteor., *25,* 1241–1254.

Estie, K. E. 1984. Forecasting the formation and movement of the coastal low. Summaries and abstracts of the Coastal Low Workshop held at Simon's Town, March, 1984, 17–27.

Franks, P. J. S. and L. J. Walstad. 1997. Phytoplankton patches at fronts: A model of formation and response to wind events. J. Mar. Res., *55,* 1–29.

Gill, A. E. 1977. Coastally trapped waves in the atmosphere. Quart. J. R. Met. Soc., *103,* 431–440.
—— 1982. Atmosphere-Ocean Dynamics, Academic Press, NY, 662 pp.
Halpern, D. 1976. Structure of a coastal upwelling event observed off Oregon during July 1973. Deep-Sea Res., *23,* 495–508.
Hunter, I. T. 1982. The coastal wind field of the southern Cape, *in* Proceedings of the Eighteenth Coastal Engineering Conference, Cape Town, South Africa, B. L. Edge, ed., American Society of Civil Engineers, NY, 2551–2561.
—— 1988. Climate and weather off Natal, *in* Coastal Ocean Studies off Natal, South Africa, E. H. Schumann, ed., Lecture Notes on Coastal and Estuarine Studies, Springer-Verlag, NY, 81–100.
Hutchings, L. 1992. Fish harvesting in a variable, productive environment—searching for rules or searching for exceptions? S. Afr. J. Mar. Sci., *12,* 297–319.
Jenkins, G. M. and D. G. Watts. 1968. Spectral Analysis and Its Applications, Holden-Day, San Francisco, 525 pp.
Jury, M. R., C. MacArthur and C. Reason. 1990. Observations of trapped waves in the atmosphere and ocean along the coast of southern Africa. S. Afr. Geogr. J., *72,* 33–46.
Largier, J. L. 1987. Internal shelf tides and wind-driven motions in deepening the surface mixed layer, PhD thesis, University of Cape Town.
Largier, J. L. and V. P. Swart. 1987. East-west variation in thermocline breakdown on the Agulhas Bank. S. Afr. J. Mar. Sci., *5,* 263–272.
Lentz, S. J. 1992. The surface boundary layer in coastal upwelling regions. J. Phys. Oceanogr., *22,* 1517–1539.
Lutjeharms, J. R. E., A. A. Meyer, I. J. Ansorge, G. A. Eagle and M. J. Orren. 1996. The nutrient characteristics of the Agulhas Bank. S. Afr. J. Mar. Sci., *17,* 253–274.
Nelson, G. and L. Hutchings. 1983. The Benguela upwelling area. Prog. Oceanogr., *12,* 333–356.
Preston-Whyte, R. A. and P. D. Tyson. 1988. The Atmosphere and Weather of Southern Africa, Oxford University Press, Cape Town, 374 pp.
Schumann, E. H. 1989. The propagation of air pressure and wind systems along the South African coast. S. Afr. J. Sci., *85,* 382–385.
—— 1998. The coastal ocean off southeast Africa, including Madagascar, *in* The Sea, A. R. Robinson and K. H. Brink, eds., *11,* 557–581.
Schumann, E. H. and L. J. Beekman. 1984. Ocean temperature structures on the Agulhas Bank. Trans. Roy. Soc. S. Afr., *45,* 191–203.
Schumann, E. H. and K. H. Brink. 1990. Coastal-trapped waves off the coast of South Africa: generation, propagation and current structures. J. Phys. Oceanogr., *20,* 1206–1218.
Schumann, E. H., A. L. Cohen and M. R. Jury. 1995. Coastal sea surface temperature variability along the south coast of South Africa and the relationship to regional and global climate. J. Mar. Res., *53,* 231–248.
Schumann, E. H. and J. A. Martin. 1991. Climatological aspects of the coastal wind field over Algoa Bay, South Africa. S. Afr. Geogr. J., *73,* 48–51.
Schumann, E. H. and L-A. Perrins. 1982. Tidal and inertial currents around South Africa, *in* Proceedings of the Eighteenth Coastal Engineering Conference, Cape Town, South Africa, American Society of Civil Engineers, NY, 2562–2580.
Schumann, E. H., L-A. Perrins and I. T. Hunter. 1982. Upwelling along the south coast of the Cape Province, South Africa. S. Afr. J. Sci., *78,* 238–242.
Schumann, E. H., G. J. B. Ross and W. S. Goschen. 1988. Cold water events in Algoa Bay and Cape south coast, South Africa, in March/April, 1987. S. Afr. J. Sci., *84,* 579–584.
Shannon, L. V. 1985. The Benguela Ecosystem Part 1. Evolution of the Benguela, physical features and processes. Oceanogr. Mar. Biol. Ann. Rev., *23,* 105–182.

Shannon, L. V., R. J. M. Crawford, D. E. Pollock, L. Hutchings, A. J. Boyd, J. Taunton-Clark, A. Badenhorst, R. Melville-Smith, C. J. Augustyn, K. L. Cochrane, I. Hampton, G. Nelson, D. W. Japp and R. J. Q. Tarr. 1992. The 1980s—a decade of change in the Benguela ecosystem. S. Afr. J. Mar. Sci., *12,* 271–296.

Swart, V. P. and J. L. Largier. 1987. Thermal structure of Agulhas Bank water. S. Afr. J. Mar. Sci., *5,* 243–254.

Tilney, R. L., G. Nelson, S. E. Radloff and C. D. Buxton. 1996. Ichthyoplankton distribution and dispersal in the Tsitsikamma National Park marine reserve, South Africa. S. Afr. J. Mar. Sci., *17,* 1–14.

Walker, N. D. 1986. Satellite observations of the Agulhas Current and episodic upwelling south of Africa. Deep-Sea Res., *33,* 1083–1106.

Welsh, J. G. 1964. Measurements of currents on the Agulhas Bank with an Ekman current meter. Deep-Sea Res., *11,* 43–52.

Received: *1 June, 1998;* revised: *19 March, 1999.*